ARTICLE
Journal of Cellular Biochemistry 114:456–470 (2013)

Journal of Cellular Biochemistry

Platycodin D Induces Anoikis and Caspase-Mediated Apoptosis via p38 MAPK in AGS Human Gastric Cancer Cells

Jaemoo Chun, Eun Ji Joo, Minseok Kang, and Yeong Shik Kim*

Natural Products Research Institute, College of Pharmacy, Seoul National University, 1 Gwanak-ro, Gwanak-gu, Seoul 151-742, Republic of Korea

ABSTRACT

Mitogen-activated protein kinases (MAPKs) cascades play important roles in cell proliferation, death, and differentiation in response to external stimuli. However, the precise role of MAPKs in platycodin D (PD)-induced cytotoxicity remains unclear. In this study, we investigated the anticancer effect of PD and its underlying mechanism on AGS human gastric cancer cells. PD significantly inhibited cell proliferation and induced anoikis, which is a form of apoptosis in which cells detach from the substrate. It showed phosphatidylserine externalization, DNA fragmentation, increase of sub-G1 phase, and activation of caspases in a dose- and time-dependent manner. This apoptosis has been associated with the extrinsic pathway via Fas-L and the intrinsic pathway via mitochondrial Bcl-2 family members. Moreover, PD led to the phosphorylation of stresses-activated protein kinases such as JNK and p38, followed by the activation of AP-1. However, pretreatment with SB203580 (a p38 specific inhibitor) suppressed PD-induced p38 and AP-1 activation, and subsequently attenuated the PD-induced apoptosis in AGS cells. These results suggest that p38 activation is responsible for PD-induced apoptosis in AGS cells and PD might be useful for the development as the anticancer agent of gastric cancer. J. Cell. Biochem. 114: 456–470, 2013.

KEY WORDS: PLATYCODIN D; APOPTOSIS; p38 MAPK; AGS; ANOIKIS; AP-1

Gastric cancer is the second leading cause of cancer-related death and the fourth most common cancer in the world [Parkin, 2001; Roder, 2002]. The highest incidence rates of gastric cancer are observed in Eastern Asia, South America, and Eastern Europe, while the incidence is low in the United States [Varadhachary and Ajani, 2005]. The current chemotherapies for gastric cancer are limited due to side effects, and targeted therapy has not been successful in the treatment of gastric cancer. Thus, the development of new agents is required [Lee et al., 2008]. More than 60% of anticancer drugs are directly or indirectly derived from natural sources [Gordaliza, 2007]. Consequently, much of the attention for developing anticancer agents has been focused on the anticancer properties of natural products and their applications, which play an important role in the prevention and treatment of cancer [Cragg et al., 2009].

Epithelial cells require adhesion to a type of extracellular matrix (ECM) for survival. Specific transmembrane receptors called integrins mediate the binding and attachment of these cells to the ECM and create focal adhesions. The loss of cell–ECM contacts results in integrant disengagement and the reorganization of the intracellular cytoskeleton [Giancotti and Ruoslahti, 1999; Li and Xu, 2000]. These events lead to changes in the expression of proteins kinases such as the inhibition of focal adhesion kinase (FAK) and c-Src or the activation of the p38 mitogen-activated protein kinase (MAPK). These changes alter the expression of proteins associated with cell survival, which are directly involved in apoptosis, a phenomenon often referred to as anoikis [Frisch and Screaton, 2001; Windham et al., 2002].

Apoptosis, or programmed cell death, is a highly regulated process that involves the activation of a series of molecular events leading to cell death. It can be induced by various stimuli, including growth factor withdrawal, irradiation, cytotoxic drugs, and death receptor ligands. It consists of two major pathways. One is the death receptor (extrinsic) pathway, which is initiated by specific ligands such as Fas-ligand (Fas-L), TNF-α, and TRAIL that activate caspase-8 [Ravindran et al., 2009]. Caspase-8 activates caspase-3 or it can

Conflict of interest: None declared.
Grant sponsor: National Research Foundation of Korea (NRF); Grant number: 20090083533.
*Correspondence to: Yeong Shik Kim, PhD, Natural Products Research Institute, College of Pharmacy, Seoul National University, 1 Gwanak-ro, Gwanak-gu, Seoul 151-742, Republic of Korea. E-mail: kims@snu.ac.kr
Manuscript Received: 29 June 2012; Manuscript Accepted: 30 August 2012
Accepted manuscript online in Wiley Online Library (wileyonlinelibrary.com): 7 September 2012
DOI 10.1002/jcb.24386 • © 2012 Wiley Periodicals, Inc.

leads to the activation of the mitochondrial pathway via the cleavage of Bid (a pro-apoptotic member of the Bcl-2 family) [Li et al., 1998]. Another apoptotic pathway is the mitochondrial (intrinsic) pathway, which is initiated by the release of cytochrome *c* from mitochondria [Arnoult et al., 2002]. The released cytochrome *c* activates caspase-9, which in turn induces the activation of caspase-3, one of the major executioner caspases. The activated caspase-3 induces the cleavage of poly (ADP-ribose) polymerase-1 (PARP1), a DNA repair enzyme, and finally leads to programmed cell death [Boulares et al., 1999].

A recent study suggested that MAPK signaling pathways play an important role in triggering apoptosis because they are often activated in response to various cellular stressors and growth factors [Chang and Karin, 2001]. Stress-activated protein kinases (SAPKs) such as c-Jun *N*-terminal kinase (JNK) and p38, together with extracellular signal-regulated kinase (ERK) comprise the family of MAPKs. The ERK pathway is associated with regulating cell survival during differentiation responses and protecting cells against apoptosis, whereas the JNK, and p38 MAPK pathways are commonly linked to promoting cell apoptosis and death [Johnson and Lapadat, 2002; Mansouri et al., 2003]. MAPKs share several upstream regulators [Wagner and Nebreda, 2009] and are involved in the regulation of transcription factors such as activator protein 1 (AP-1) to induce biological changes, including cell proliferation, apoptosis, and differentiation [Silvers et al., 2003; Giuliano et al., 2006].

Platycodin D (PD) is a triterpenoid saponin mainly found in the root of *P. grandiflorum* (Companulaceae). Recently, various pharmacological activities of PD have been reported, such as anti-inflammation [Wang et al., 2004; Ahn et al., 2005], immunogenicity, anti-adipogenesis [Lee et al., 2010], a cholesterol-lowering effect [Zhao et al., 2006], and apoptosis of leukemia cells [Kim et al., 2008ab; Shin et al., 2009], keratinocytes [Ahn et al., 2006], and breast cancer cells [Yu and Kim, 2010], but the exact mechanism of action has not been clarified in AGS cells. In the present study, we found that PD greatly potentiated the apoptotic effect on AGS human gastric cancer cells in various cancer cell lines, and we examined its molecular mechanism of apoptosis induction in AGS cells. In addition to the apoptotic effect, the possible effect of PD in the activation of p38 MAPK, and AP-1 transcription factor was investigated.

MATERIALS AND METHODS

CHEMICALS AND REAGENTS

PD was isolated from the root of *Platycodon grandiflorum* using high-speed counter current chromatography as described, previously [Ha and Kim, 2009]. The purity of the PD was measured using HPLC and determined to be over 99% (Fig. 1A). PD was dissolved in dimethyl sulfoxide (DMSO) to obtain a stock solution and the DMSO concentration was kept below 0.05% in the cell cultures so that it had no effect on the cells. Dulbecco's phosphate buffered saline (DPBS), DMSO, a protease inhibitor cocktail, 4,6-diamidino-2-phenylindole (DAPI), 3-(4,5-dimethylthiazol-2-yl)-2,5-diphenyltetrazolium bromide (MTT), 5,5′,6,6′-tetrachloro-1,1′,3,3′-tetraethylbenzimidazolylcarbocyanine chloride (JC-1), the JNK inhibitor SP600125, the p38 inhibitor SB203580 and the ERK1/2 inhibitor U0126 were purchased from Sigma Chemical Co. (St. Louis, MO). Annexin V-FITC and a propidium iodide (PI) kit were acquired from BD Biosciences (San Diego, CA). Primary antibodies for caspase-3, caspase-8, caspase-9, PARP1, p-p38, p-JNK, p-ERK, p38, JNK, ERK, Fas-L, Fas, Bax, Bcl-2, and β-actin and all secondary antibodies were from Santa Cruz Biotechnology (Santa Cruz, CA). Primary antibodies for FAK, Bid, Survivin, cytochrome *c*, c-Jun, and Bim were from Epitomics (Burlingame, CA). Penicillin, streptomycin, DMEM (high glucose), RPMI 1640 medium and fetal bovine serum (FBS) were obtained from GenDepot (Barker, TX). All other chemicals were purchased from Sigma Chemical Co. unless otherwise specified.

CELL CULTURE

AGS human gastric cancer cells, A549, and H460 human lung cancer cells, HepG2 human hepatoma cells, and Jurkat human T cell leukemia cells were obtained from the American Type Culture Collection (Rockville, MD). MCF-7 human breast cancer cells, Caco-2 human colon cancer cells, HeLa human cervical cancer cells, and Panc-1 human pancreatic cancer cells were obtained from the Korea Cell Bank (Seoul, Korea). MRC-5 human lung normal cells, MCF-10A human breast normal cells, and Chang human hepatic normal cells were obtained from the American Type Culture Collection. AGS, A549, H460, and Jurkat cells were maintained in RPMI 1640 medium, and HepG2, MCF-7, Caco-2, HeLa, Panc-1, MRC-5 and Chang cells were maintained in DMEM medium supplemented with 10% FBS and antibiotics (penicillin 100 U/ml, and streptomycin 100 μg/ml). MCF-10A were maintained in DMEM medium supplemented with 10% FBS, 20 ng/ml epidermal growth factor (Sigma), 500 ng/ml hydrocortisone (Sigma), and antibiotics (penicillin 100 U/ml, and streptomycin 100 μg/ml). Cultures were maintained in a humidified atmosphere incubator at 37°C in 5% CO_2.

CELL VIABILITY ASSAY

The cell viability was evaluated using an MTT assay. Cells were seeded into 96-well plates at a density of 1×10^4 cells per well and stabilized at 37°C for 24 h. PD at different concentrations (6, 12, 18, 24, 30, and 60 μM) was added to each well, and then the cells were incubated for 0–48 h. The MTT solution (0.5 mg/ml) was added to each well, and the cells were incubated for another 3 h. The formazan crystals were dissolved in 100 μl of DMSO. Cell viability was assessed by measuring the absorbance at a 540 nm wavelength using an EMax Microplate Reader (Molecular Devices, Sunnyvale, CA).

OBSERVATION OF CELL MORPHOLOGY AND DAPI STAINING

AGS cells were plated in 12-well plates and incubated at 37°C for 24 h. The cells were then treated with PD (12 and 24 μM) for the indicated times and washed with DPBS before being fixed with 70% ethanol for 15 min. After the fixed cells were washed with DPBS, they were stained with DAPI (2 μg/ml) for 15 min. Subsequently, the cells were re-washed with DPBS. Cells were viewed under a CKX41 fluorescence microscope (Olympus, Tokyo, Japan) at a magnification of 400×.

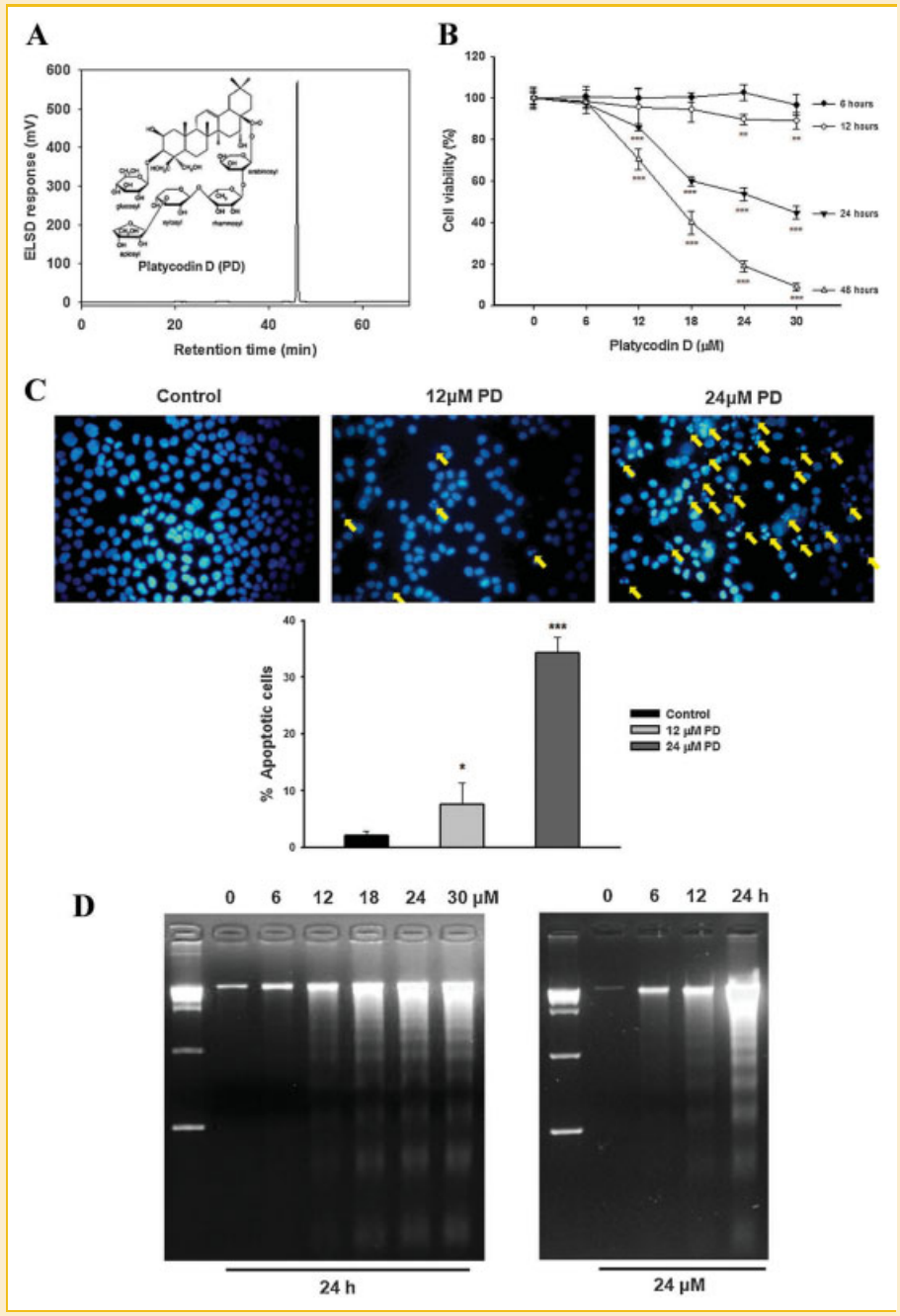

Fig. 1. Effects of PD on cell viability and apoptosis in AGS cells. A: The chemical structure of PD and HPLC analysis of the purity of PD used in the present study. B: The anti-proliferative effect of PD in AGS cells. Cells were treated with the indicated concentrations of PD (μM) for 6–48 h. Viability was determined using the MTT assay. The results are presented as the mean ± SD of three independent experiments. $^{**}P < 0.01$, and $^{***}P < 0.001$ indicate the significance compared to the vehicle-treated control. C: Nuclear morphological alterations after 24 h PD treatment as revealed by DAPI fluorescence staining. AGS cells treated with 12 and 24 μM PD were fixed with 70% ethanol, stained with 2 μg/ml DAPI solution, and detected using a fluorescence microscope. The occurrence of apoptosis was quantified as the percentage of the cells showing condensed or fragmented nuclei (arrows). $^{*}P < 0.01$, and $^{***}P < 0.001$ indicate the significance compared to the vehicle-treated control. D: The DNA fragmentation in AGS cells after PD treatment. Cells were treated with the indicated concentrations of PD for 24 h and with 24 μM PD for the indicated times. The DNA was extracted and analyzed electrophoretically on a 2% agarose gel containing ethidium bromide.

DNA FRAGMENTATION ASSAY

AGS cells were plated in 6-well plates and incubated at 37°C for 24 h. The cells were then treated with the indicated concentrations of PD for 24 h and with 24 μM PD for the indicated times. Adherent and floating cells were collected and washed with DPBS. The cells were lysed with Triton X-100 lyses buffer (40 ml of 0.5 M EDTA; 5 ml of 1 M Tris–Cl buffer; pH 8.0; 5 ml of 100% Triton X-100; 50 ml of H_2O) and incubated for 30 min on ice before centrifugation. The DNA was extracted using a 25:24:1 (v/v/v) equal volume of neutral phenol:chloroform:isoamyl alcohol and precipitated in two

equivalent volumes of cold ethanol and a one-tenth volume of sodium acetate. The DNA pellets were centrifuged, washed with 70% ethanol, briefly dried, and resuspended in the RNase a solution. All DNA was analyzed electrophoretically on a 2% agarose gel containing ethidium bromide. The gel was visualized under a UV transilluminator.

ANNEXIN V/PI STAINING

Apoptotic cells were differentiated from viable or necrotic cells using a combined staining of Annexin V-FITC, and PI. Adherent and floating cells were collected and washed with DPBS and subsequently centrifuged. The cells were suspended in 1× binding buffer and stained with Annexin V-FITC and PI. After incubation for 15 min at room temperature in the dark, the cells were analyzed with flow cytometry (Coulter EPICS XL, Beckman Coulter Inc., CA).

CELL CYCLE ANALYSIS

The effect of PD on AGS cell cycle phase distribution was assessed using flow cytometry. Briefly, cells were seeded in 6-well plates and incubated for 24 h. After treatment with PD, cells were collected by trypsinization and washed with DPBS. Then, cells were fixed with 70% ethanol and incubated at −20°C overnight. The cells were then collected by centrifugation. The pellet was washed, suspended in DPBS and incubated with RNase A (50 μg/ml) at room temperature for 30 min. The cells were stained with PI (50 μg/ml) for 10 min, and the DNA content was measured with flow cytometry and analyzed using EXPO32 ADC software.

JC-1 MITOCHONDRIAL MEMBRANE POTENTIAL ASSAY

The mitochondrial membrane potential was assessed using JC-1 dye. The JC-1 dye forms aggregates in intact mitochondria that emit red fluorescence. However, when the mitochondrial membrane potential is disrupted by apoptosis, mitochondrial aggregates do not form, and the dye remains in the monomeric form in the cytoplasm, emitting green fluorescence. The cells were plated at 5×10^4 cells per well in 24-well plates and incubated for 24 h. PD was added to the cells, and the cells were incubated for 24 h. The cells were subsequently incubated with JC-1 dye diluted in RPMI 1640 medium for 30 min at 37°C and finally, observed using a CKX41 fluorescence microscope.

PREPARATION OF CYTOSOLIC EXTRACTS

After treatment with PD for 24 h, sub-cellular fractions were prepared to examine the cytochrome *c* release from mitochondria. Briefly, cells were collected, washed, and resuspended in 100 μl of ice-cold buffer (250 mM sucrose, 20 mM HEPES [pH 7.9], 10 mM KCl, 1.5 mM $MgCl_2$, 1 mM EDTA, 1 mM DTT, 1 mM PMSF). After 30 min incubation on ice, the protein in the isolated cytosolic fractions was analyzed by Western blotting for cytochrome *c*.

FAS-LIGAND DETECTION BY FLOW CYTOMETRY

The cell surface expression of Fas-L was assessed by immunofluorescence flow cytometry. In brief, cell were treated with 24 μM PD for 24 h, washed with DPBS, and stained with 5 μl of anti-human Fas-L-PE (eBioscience, San Diego, CA) or isotype control antibody for 30 min on ice. After being washed twice in DPBS, the cells were analyzed using flow cytometry on the FL-2 channel.

RT-PCR ANALYSIS

AGS cells were incubated with PD for 24 h. Total RNA was extracted using the Easy-Blue™ Total RNA Extraction Kit (Intron Biotechnology, Korea). RT-PCR was performed using the ONE-STEP RT-PCR PreMix kit™ (Intron Biotechnology, KOREA) for 30 cycles with each cycle consisting of 1 min at 94°C, 1 min at 55°C 1 min, and 1 min at 72°C. The primers used for amplification of the Fas-L were sense 5′-CAACTCAAGGTCCATGCCTC-3′ and antisense 5′-AGATTCCT-CAAAATTGACCAG-3′; for Fas were sense 5′-GACAAAGCC-CATTTTTCTTCC-3′, antisense 5′-ATTTATTGCCACTGTTTCAGG-3′; and for GAPDH were sense 5′-GGTCGGAGTCAACGGATTTGGTCG-3′, antisense 5′-CTTCCGACGCCTGCTTCACCAC-3′. The RT-PCR products were separated by electrophoresis using a 2% agarose gel stained with ethidium bromide, and the gels were viewed using a UV transilluminator.

WESTERN BLOTTING

AGS cells were seeded at a density of 4×10^5 cells per well in 6-well plates and attached for 24 h. After incubation with PD at various concentration and times, the adherent and floating cells were collected, washed with DPBS and centrifuged. The pellet was resuspended in 50–80 μl of lyses buffer (20 mM HEPES [pH 7.6], 350 mM NaCl, 20% glycerol, 0.5 mM EDTA, 0.1 mM EGTA, 1% NP-40, 50 mM NaF, 0.1 mM DTT, 0.1 mM PMSF) including a protease inhibitor cocktail and incubated on ice for 30 min with intermittent mixing. The extract was centrifuged at 15,000 rpm for 10 min at 4°C. The protein concentration was estimated using a Bradford reagent (Bio-Rad Laboratories Inc., CA). An equal amount (20–30 μg) of protein was loaded on 10% or 12% SDS–polyacrylamide gels and transferred using a semi-dry method to a nitrocellulose membrane. After blocking with 5% skim milk, the membrane was incubated at 4°C overnight with specific primary antibodies. The membrane was washed and incubated at room temperature for 1 h with secondary antibodies conjugated with horseradish peroxidase (HRP). Finally, the immunoblot was developed for visualization using a chemiluminescence kit (AbFrontier, Seoul, Korea). The intensity of each band was quantitatively determined using the UN-SCAN-IT™ software (Silk Scientific, UT).

RNA INTERFERENCE

Knockdown of human p38-alpha MAPK expression was performed by RNA interference methods using small interfering RNAs (siRNAs). AccuTarget Negative control siRNA (Bioneer, Daejeon, Korea) was used as a control scrambled siRNA. The siRNAs specific for p38-alpha MAPK (siRNA No. 1092108) were obtained from Bioneer. AGS cells were transfected with control-scrambled siRNA or p38-alpha MAPK siRNA at the indicated concentrations using Lipofectamine 2000 (Invitrogen, Carlsbad, CA) as recommended by the manufacturer.

ELECTROPHORETIC MOBILITY SHIFT ASSAY (EMSA)

To investigate the inhibitory effect of PD on AP-1 DNA binding, an EMSA was performed as previously described [Shin et al., 2010].

Briefly, nuclear extracts prepared from AGS cells were incubated with a ^{32}P-end-labeled 22-mer double-stranded AP-1 consensus oligonucleotide (Promega, CA) with the sequence 5′-CGCTTGATGAGTCAGCCGGAA-3′ or NF-κB consensus oligonucleotide with the sequence 5′-AGTTGAGGGGACTTTCCCAGGC-3′ for 30 min at room temperature, and the DNA–protein complexes were electrophoresis through 6% native polyacrylamide gels. Finally, the gels were dried, and the signals obtained from the dried gel were quantitated using an FLA-3000 apparatus (Fuji, Tokyo, Japan) with the BAS reader version 3.14 and Aida version 3.22 software (Fuji-Raytest, Straubenhardt, Germany).

STATISTICAL ANALYSIS

The results are expressed as the mean ± standard deviations (SD) from three different experiments. A one-way analysis of variance (ANOVA) followed by Dunnett's *t*-test was applied to assess the statistical significance of the differences between the study groups (SPSS version 10.0, Chicago, IL). A value of $P < 0.05$ was chosen as the criterion for statistical significance.

RESULTS

THE ANTI-PROLIFERATIVE EFFECT OF PD IN HUMAN CANCER CELL LINES

We first compared the effects of PD on the viability of various human cell lines using the MTT assay. As shown in Table I, PD had a dose-dependent cytotoxic effect in human cancer cells. AGS, A549, Caco-2, and HepG2 cells were more sensitive to PD than the other cell lines. However, PD at the concentration up to 50 μM did not affect the survival of human normal cell lines such as MRC-5, MCF-10A, and Chang cells. In AGS, A549, Caco-2, and HepG2 cells indicating the relatively high cytotoxic, the ratio of cells in the sub-G1 phase was analyzed with flow cytometry to investigate the induction of apoptosis. PD had the strongest apoptosis-inducing effect on AGS cells. As a result, we further examined the mechanism through which PD induces apoptosis in AGS cells.

TABLE I. IC_{50} Values for PD on the Growth and the Ratio of Sub-G1 Phase Cells in Various Human Cell Lines

Cell line	Origin	IC_{50} (μM)	Sub-G1 phase ratio (%) 0	12 (μM)	24 (μM)
AGS	Gastric carcinoma	25.6	4.39	14.96	54.17
A549	Lung carcinoma	22.2	2.62	3.47	10.46
MRC-5	Lung normal cells	>60	n.d.	n.d.	n.d.
H460	Lung carcinoma	33.8	n.d.	n.d.	n.d.
Caco-2	Colon carcinoma	24.6	3.90	3.17	9.37
MCF-7	Breast carcinoma	38.5	n.d.	n.d.	n.d.
MCF-10A	Breast normal cells	>60	n.d.	n.d.	n.d.
Jurkat	Leukimia	58.8	n.d.	n.d.	n.d.
HepG2	Hepatocarcinoma	29.0	2.97	3.40	3.77
Chang	Hepatic normal cells	>60	n.d.	n.d.	n.d.
HeLa	Cervix carcinoma	52.1	n.d.	n.d.	n.d.
PANC-1	Pancreatic carcinoma	33.6	n.d.	n.d.	n.d.

IC_{50} value for PD was assessed with an MTT assay. The percentage of cells in the sub-G1 phase was calculated using flow cytometric analysis. n.d., not determined.

PD INDUCES THE NUCLEAR CONDENSATION AND DNA FRAGMENTATION IN AGS CELLS

PD did not affect AGS cell viability for 12 h. However, after 24 h, PD significantly inhibited cell proliferation and induced cytotoxic effects in a dose- and time-dependent manner (Fig. 1B). To characterize the PD-induced growth inhibition, we observed the morphological and nuclear changes in AGS cells. Cells treated with 12 and 24 μM PD showed typical characteristics of apoptosis such as cell shrinkage, membrane blabbing, apoptotic bodies, and fragmented nuclei detected by fluorescence microscope (Fig. 1C). Distinctive DNA fragmentation ladders were also observed in PD-treated cells in a dose- and time-dependent manner (Fig. 1D). These results suggest that PD is able to induce apoptotic cell death in AGS cells.

FLOW CYTOMETRIC ANALYSIS OF APOPTOSIS

For the quantitative investigation of PD on apoptosis, the exposure of phosphatidylserine (PS), a marker of early apoptosis, to the cell surface was assessed using flow cytometry. Compared to the control group, PD triggered early apoptosis in AGS cells in a dose- and time-dependent manner. Approximately 40.2% of the cells were in early apoptosis in the 30 μM PD-treated group after 24 h, compared with 6.1% of the vehicle-treated group (Fig. 2A). Additionally, treatment with 24 μM PD for 48 h induced early/late apoptosis in approximately 38.5% of cells (Fig. 2B). The total DNA content of AGS cells was also analyzed using flow cytometry. Treatment with a higher concentration of or a longer exposure to PD dramatically increased the proportion of cells in the sub-G1 phase, indicative of apoptotic peaks in a dose- and time-dependent manner. These results indicate that PD induces apoptosis in dose- and time-dependent manners in AGS cells.

PD INDUCES CELL DETACHMENT, FOLLOWED BY APOPTOSIS

FAK is a key mediator of integrin signaling and a component of cell-substratum adhesions, known as focal adhesion complexes. FAK plays an important role in the maintenance of cell survival, and the disruption of FAK signaling results in a loss of substrate adhesion and anoikis in adherent cells [Park et al., 2009; Zouq et al., 2009]. In the cell viability assay, we examined the plates under a microscope for any possible changes in cell morphology following PD treatment. We observed that PD treatment led to cell rounding followed by detachment from the plate (Fig. 3A), suggesting that PD might cause anoikis-like apoptotic cell death, possibly by reducing cellular adhesion to the ECM by altering FAK levels. Accordingly, we assessed the level of FAK. As shown in Figure 3B, PD treatment resulted in a time- and dose-dependent decrease in the FAK protein level. In addition, DNA fragmentation was examined to determine whether the apoptotic effect is associated with detachment in PD-treated AGS cells. Interestingly, fragmented DNA was not observed in adherent cells, while most of the detached cells showed signs of induced apoptosis (Fig. 3C). These results demonstrate that PD induced cell detachment followed by anoikis.

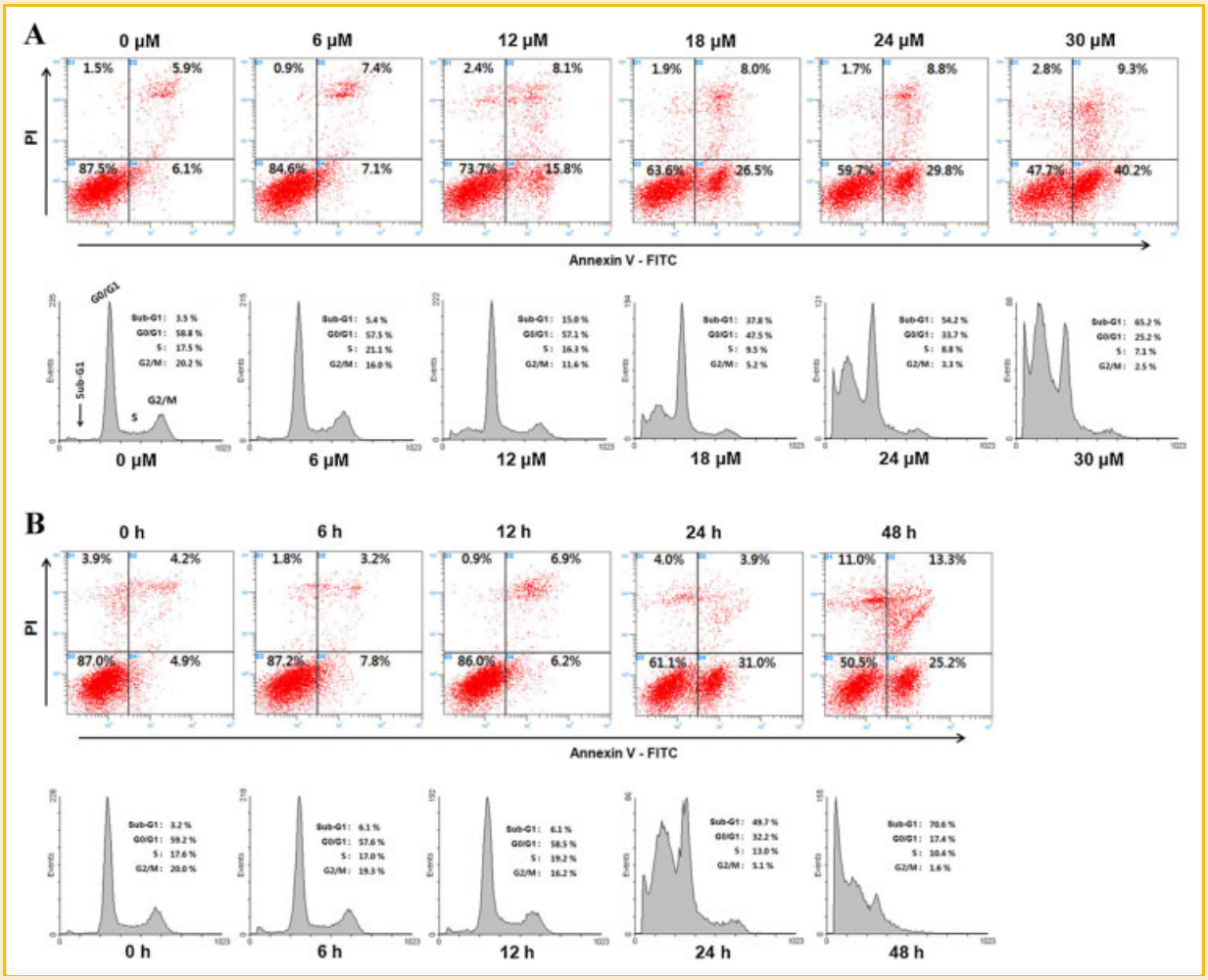

Fig. 2. Flow cytometric analysis of PD-induced apoptosis in AGS cells. Upper panel shows the flow cytometric analysis of PD-treated AGS cells after Annexin V-FITC antibody binding and propidium iodide uptake. The lower-right quadrant represents early apoptosis, and the upper-right quadrant represents late apoptosis. The lower panel shows the cell cycle analysis to evaluate the ratio of cells in the sub-G1 phase. The results were determined using a flow cytometry in which 20,000 events were counted per sample. A: AGS cells were treated with the indicated concentrations of PD for 24 h. B: AGS Cells were treated with 24 μM of PD for 6–48 h and subsequently analyzed with flow cytometry. The results shown are representative of three independent experiments.

PD LEADS TO THE EXPRESSION OF APOPTOSIS-RELATED PROTEINS AND THE ACTIVATION OF CASPASES

To further demonstrate that the anti-proliferative effect of PD was due to apoptosis, proteins implicated in apoptosis were evaluated using Western blotting. As shown in Figure 3D, the exposure of AGS cells to PD resulted in the cleavage of PARP, an increase in caspase-8 and caspase-3, and a decrease in procaspase-9, which is consistent with the presence of fragmented DNA. These events were time- and dose-dependent, but p53- and p21-independent (Fig. 3E).

INVOLVEMENT OF BOTH EXTRINSIC AND INTRINSIC PATHWAYS IN PD-INDUCED APOPTOSIS

To clarify the mechanism of PD-induced apoptosis in AGS cells, we further examined the activity of extrinsic pathway, specifically with regard to Fas-L and Fas. The results showed that in AGS cells, PD increased the mRNA and protein expression of Fas-L, but not Fas (Fig. 4A). The cell surface expression of Fas-L was also confirmed by immunofluorescence flow cytometry with anti-Fas-L-PE after PD treatment (Fig. 4B). Therefore, increase in Fas-L expression by PD is responsible for apoptosis in AGS cells, which occurs through the activation of a caspase-8 driven extrinsic pathway. To investigate whether intrinsic pathway was involved in PD-induced cell death, we determined the levels of the anti-apoptotic protein Bcl-2 and the pro-apoptotic protein Bax. The ratio of Bax/Bcl-2 was increased by PD treatment, which indicates the triggering of the mitochondrial apoptotic pathway (Fig. 4C). Mitochondria dysfunctions, including the loss of mitochondrial membrane potential, have been proposed as one of the early events during apoptotic cell death [Liu et al., 2004]. We, therefore, assessed the change in mitochondrial membrane potential using the mitochondria-specific JC-1 dye. In control cells with high-mitochondrial membrane potential, JC-1 formed aggregates with red fluorescence. However, in cells treated with 24 μM PD, JC-1 remained in the

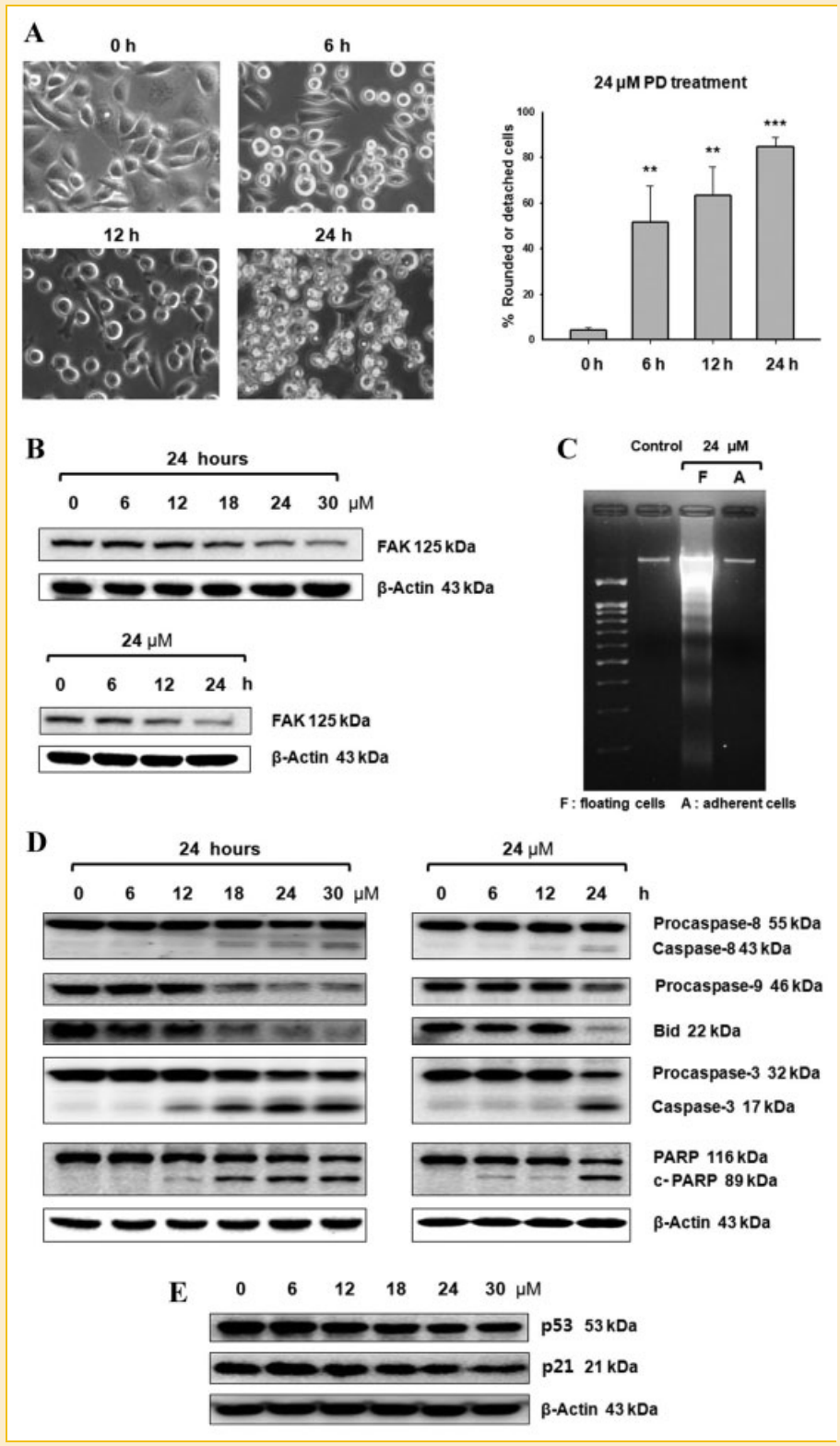

Fig. 3. PD induced detachment of AGS cells followed by anoikis-like apoptotic cell death. A: AGS cells were treated with 24 μM PD for 6–24 h. The cells displaying rounded and detached morphology were counted and quantified as the percentage of the cells showing rounded and detached cells. $^{**}P < 0.01$, and $^{***}P < 0.001$ indicate the significance compared to the vehicle-treated control. B: AGS cells were treated with the indicated concentrations of PD for 24 h, and with 24 μM of PD for 6–24 h. Cell lysates were prepared and subjected to SDS–PAGE and Western blotting to determine the FAK protein level. In all Western blotting experiments, β-actin was used as a loading control. C: After treatment with 24 μM PD for 24 h, cells were divided into adherent and floating cells, and a DNA fragmentation assay was employed to determine whether the apoptotic effect is associated with detachment. D: PD induced apoptosis through a caspase-dependent pathway. Western blotting was performed using PARP1, caspase-3, Bid, caspase-8, and caspase-9 antibodies. E: The protein levels of p53, and p21 were analyzed by Western blotting. The results shown are representative of three independent experiments.

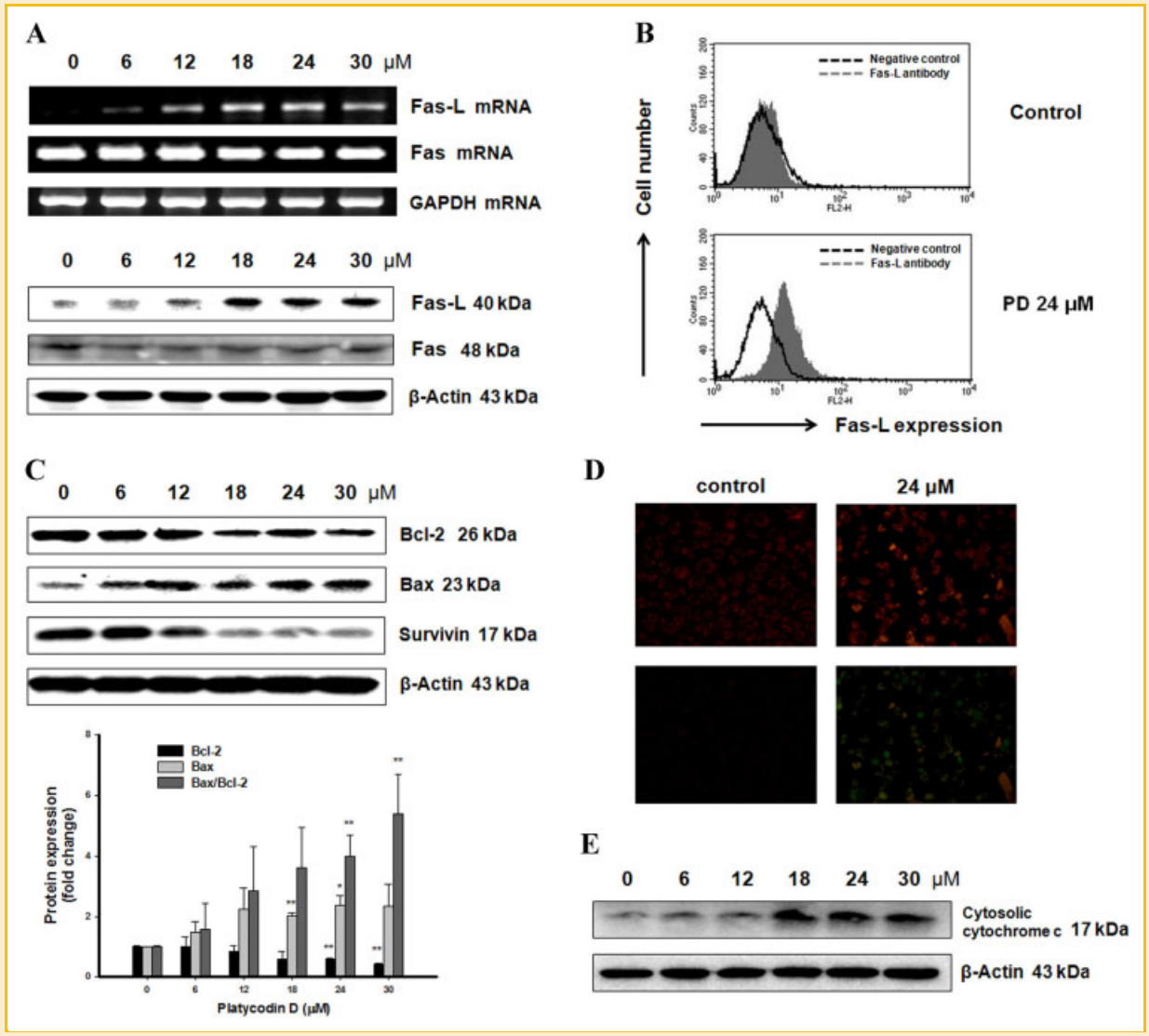

Fig. 4. Involvement of both the extrinsic pathway and intrinsic pathway in PD-induced apoptosis. A: The protein and mRNA expression of Fas-L, and Fas in AGS cells. Cells were treated with the indicated concentrations of PD for 24 h. The levels of Fas-L, and Fas protein were determined by Western blotting. Total RNA was immediately extracted and processed for RT-PCR analysis using specific gene primers. For quantification, the mRNA expression data were normalized to the GAPDH signal. B: Flow cytometric analysis of membrane-bound Fas-L expression. AGS cells were stained with anti-Fas-L or isotype control antibody. Unshaded and shaded peaks correspond to control and specific staining, respectively. C: Alteration of Bcl-2 family protein levels in PD-treated AGS cells. AGS cells were treated with the indicated concentrations of PD for 24 h. The cells were then harvested and prepared for the detection of Bcl-2, Bax and surviving protein expression using Western blotting. The ratio of Bax/Bcl-2 was calculated, and these results are presented as the mean ± SD of three independent experiments. $^{*}P < 0.05$, and $^{**}P < 0.01$ indicate the significance compared to the vehicle-treated control. D: Loss of mitochondrial membrane potential in PD-treated AGS cells. Cells were incubated with JC-1 fluorescence dye and observed using a fluorescence microscope. E: PD induced cytochrome c release from the mitochondria into the cytosol. The cytosolic lysate was prepared, and the expression of cytochrome c was determined using Western blotting. The results shown are representative of three independent experiments.

monomeric form, which emits green fluorescence (Fig. 4D). We further investigated the release of cytochrome *c* from mitochondria, which is associated with the intrinsic pathway. As shown in Figure 4E, the cytochrome *c* protein level was increased after the treatment of AGS cells with different concentrations of PD for 24 h. Taken together, these results suggest that PD is associated with not only the extrinsic pathway being initiated by Fas-L but also the intrinsic pathway via mitochondrial Bcl-2 family members.

EFFECT OF JNK, p38 AND ERK INHIBITORS ON PD-INDUCED MAPK PATHWAY ACTIVATION

We next examined the effect of PD on MAPK signaling. As shown in Figure 5A, the phosphorylation of p38 and JNK were increased after PD treatment in a dose- and time-dependent manner, but the phosphorylation of ERK was decreased. However, PD showed no effect on the total expression levels of p38, JNK, and ERK. The p38 MAPK and JNK signaling pathways have been shown to affect AP-1 activity, which is a downstream target of MAPK and an important

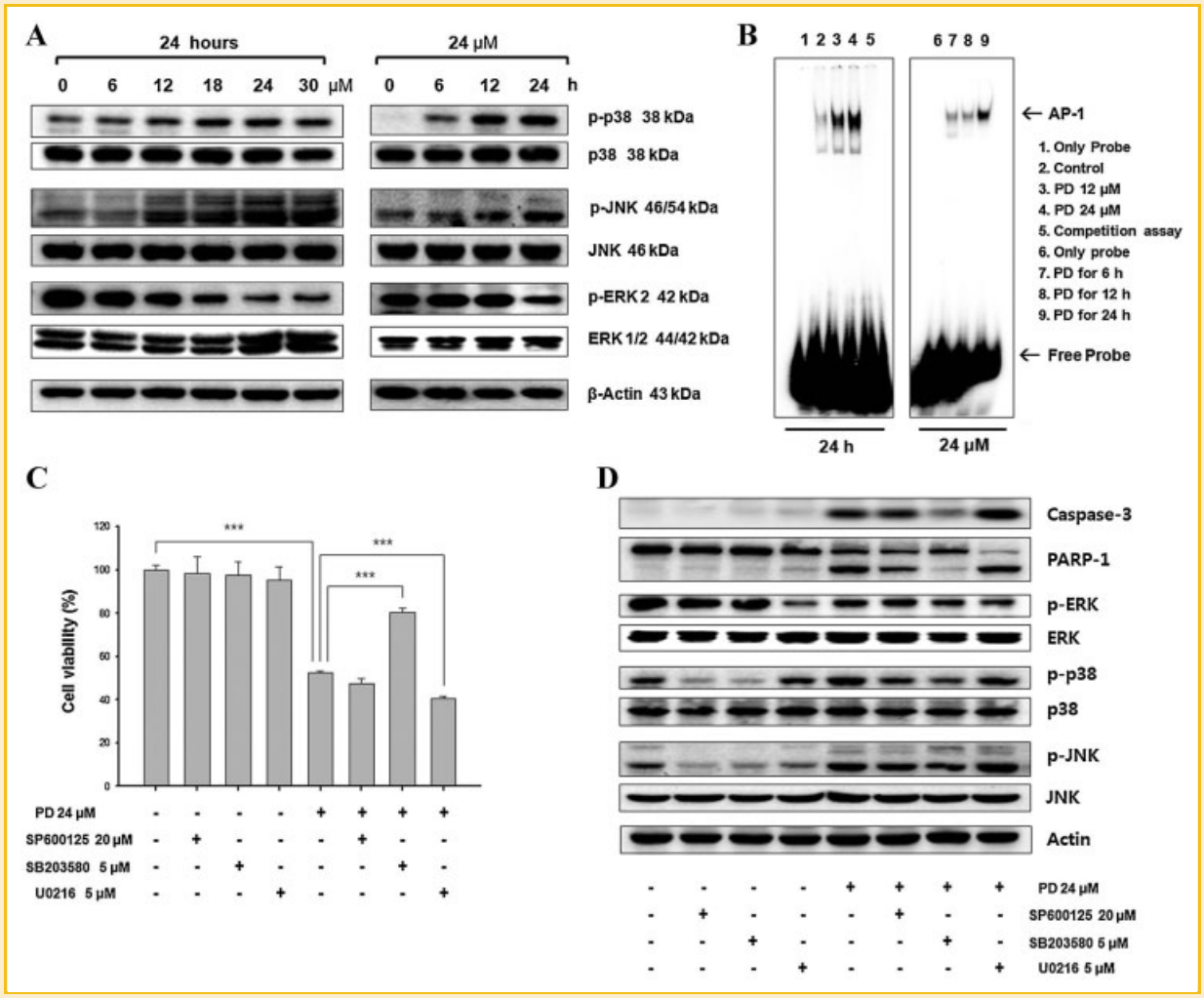

Fig. 5. Effects on MAPKs and AP-1 in the PD-treated AGS cells. A: The PD-induced activation of p38 and JNK and the inactivation of ERK in a dose- and time-dependent manner. AGS cells were treated with the indicated concentrations of PD for 24 h, and with 24 μM of PD for 6–24 h. Cell lysates were prepared and subjected to SDS–PAGE and Western blotting with antibodies against phosphorylated-p38, p38, phosphorylated-JNK, JNK, phosphorylated-ERK, and ERK. B: Effects of PD on AP-1 DNA-binding activity. The nuclear extracts prepared from AGS cells were incubated with a ^{32}P-labeled AP-1 consensus oligonucleotide and electrophoresed on a 6% polyacrylamide gel. C: The effects of pretreatment with selective MAPK inhibitors on PD-induced cell death. AGS cells were pretreated with a JNK inhibitor, an ERK inhibitor, and a p38 inhibitor followed by PD treatment for 24 h. The survival rate was measured using an MTT assay. The results are presented as the mean ± SD of three independent experiments. $^{***}P < 0.001$ indicate the significance compared to the vehicle-treated control or PD-treated group. D: The effects of pretreatment with MAPK inhibitors on the activation of caspase-3 and PARP1 and MAPK proteins in PD-treated AGS cells. The protein expression levels were determined using Western blotting. The results shown are representative of three independent experiments.

regulatory protein involved in cell growth and apoptosis [Tanos et al., 2005; Lee et al., 2010; Yan et al., 2011]. To investigate the effect of PD on the activation of AP-1, EMSA was performed. The results indicate that PD increased the DNA-binding activity of AP-1 (Fig. 5B).

To further determine whether the phosphorylation of MAPK family members is associated with PD-induced apoptosis, the AGS cells were pretreated with the JNK inhibitor SP600125 (20 μM), the p38 inhibitor SB203580 (5 μM), or the ERK inhibitor U0126 (5 μM). The survival graph showed that the inhibition of p38 MAPK rescued the viability of AGS cells, while the ERK inhibitor synergistically inhibited the cell viability, and the JNK inhibitor had no effect on viability (Fig. 5C). These observations suggest that p38 plays an important role in regulating the AGS cell death and is involved in PD-induced apoptosis. Therefore, we investigated the changes in caspase-3 and PARP1 proteins, the marker protein of apoptosis, to determine the relationship between the MAPK signaling pathway and apoptosis. Western blotting results showed that pretreatment with SB203580 suppressed the activation of caspase-3 and PARP1 by treatment with 24 μM PD. Furthermore, we observed that pretreatment with U0126 increased the activity of caspase-3 and PARP1, but SP600125 had no effect (Fig. 5D). These results suggest that p38 MAPK signaling activation plays an important role in PD-mediated apoptosis.

PD-INDUCED APOPTOSIS INVOLVES THE ACTIVATION OF p38 MAPK AND AP-1 IN AGS CELLS

To further analyze whether p38 activation plays a major role in PD-induced apoptosis, Annexin V/PI binding and the ratio of sub-G1 phase were examined. Pretreatment with SB203580 completely inhibited PD-induced apoptosis (Fig. 6A). Moreover, SB203580 reduced the up-regulation of Bax and Fas-L and restored the down-regulation of Bcl-2 in response to PD, which resulted in a reduction of caspase-8 and caspase-9 activation (Fig. 6B). We then knocked down p38 expression by transfecting AGS cells with siRNAs selectively targeting p38-alpha MAPK for 48 h. As shown in Figure 6D, p38 MAPK knockdown markedly attenuated the cell death. Next, we analyzed the effect of p38 knockdown on protein levels of apoptosis-related factors. As shown in Figure 6E, the p38 MAPK protein level was reduced and the level of phosphorylated p38 MAPK was also diminished after PD treatment. The activation of caspase-3, caspase-8, caspase-9, and PARP by PD was then suppressed.

To characterize the activation of AP-1 via the p38 MAPK in response to PD treatment, the effect of pretreatment with SB203580 was evaluated. As shown in Figure 6C, PD-mediated AP-1 activation was completely inhibited by pretreatment with SB203580. This result indicates that AP-1 activation by PD treatment is mediated through the p38 pathway. Taken together, these results demonstrate that p38 MAPK and AP-1 activation play a major role in the PD-mediated apoptosis of AGS cells.

PD INCREASES THE EXPRESSION OF AP-1 TARGET GENES

To ascertain the mechanism by which AP-1 activation increases the levels of some factors associated with apoptosis, we examined the AP-1 transcriptional targets such as c-Jun and Bim. As shown in Figure 7A, PD dose-dependently increased the expression of Bim and c-Jun. These results suggested that the pro-apoptotic action of AP-1 was involved in the expression of Bim and c-Jun with the induction of Fas-L. In addition, AGS cells were pretreated with or without 5 μM parthenolide (inhibitor of AP-1 activation) for 1 h, followed by treatment with 24 μM PD. However, parthenolide suppressed the increase in the level of c-Jun and Bim in response to PD (Fig. 7B). EMSA results also revealed that parthenolide inhibited the activation of AP-1 by PD (Fig. 7C). Therefore, these results suggest AP-1 activation is responsible for the increased expression of c-Jun and Bim.

We next investigated whether PD modulates NF-κB DNA-binding activity in AGS cells since NF-κB activation plays a crucial role in the induction of apoptosis in HaCaT by PD [Ahn et al., 2006]. Nuclear extracts were incubated with a ^{32}P-labeled NF-κB consensus oligonucleotide and subjected to EMSA. The results revealed that PD inhibited NF-κB DNA-binding activity at 24 h compared to control (Fig. 7D). The specificity of NF-κB binding to the DNA consensus sequence was confirmed by competition assay with 100-fold excess of unlabeled oligonucleotide. These results indicate that NF-κB signaling pathway is aberrantly activated in AGS cells and NF-κB activation is independent of apoptosis.

DISCUSSION

Cellular regulatory mechanisms normally maintain a balance between cell proliferation, adhesion, death and differentiation. An imbalance in the modulation of these functions leads to the development of malignant cells and tumor metastasis [Fulop and Larbi, 2002]. Based on the understanding of bioactive compounds from natural sources with respect to the regulation of cell functions [Chin et al., 2006], the development of compounds that selectively and potently induce programmed cell death in cancer cells is one of the ultimate aims in studies on cancer chemoprevention and chemotherapy [Ghobrial et al., 2005]. Various anticancer agents used in cancer chemotherapy such as pacritaxel, 5-FU, cisplatin, doxorubicin, and camptothecin have apoptosis-inducing activity [Kaufmann and Earnshaw, 2000]. Therefore, a chemical agent that has strong apoptosis-inducing activity but minimal toxicity would be expected to have especially strong potential as a new anticancer drug [Naka et al., 2002]. In the present study, we demonstrated that PD effectively induced anoikis and caspase-mediated apoptosis in AGS cells. In particular, the present study is the first to specifically elucidate that the phosphorylation of p38 contributes to the PD-mediated apoptosis in AGS cells. In the test for anti-proliferation and apoptosis on a number of human cell types, we found that PD induced strong apoptotic effects in AGS cells, while PD exhibited obvious cytotoxicity to other cancer cells. Specifically, PD exhibited potent growth inhibition and strong cytotoxicity against various human cancer cell lines (A549 lung cancer cells, $IC_{50} = 22.2$ μM; AGS gastric cancer cells, $IC_{50} = 25.6$ μM; Caco-2 colon cancer cells, $IC_{50} = 24.6$ μM; HepG2 liver cancer cells, $IC_{50} = 29.0$ μM). However, the ratio of cells in the sub-G1 phase, a hallmark of apoptosis, in PD-treated AGS cells was highly increased (12 μM PD = 14.96%; 24 μM PD = 54.17% in AGS cells) compared to other cell lines (Table I). In addition, it was interesting that PD at the concentrations mentioned above hardly affected the viability of normal cells, suggesting a selective anti-cancer activity of PD to some degree. We hypothesized that PD could be a promising candidate as an effective and less toxic chemotherapeutic agent for gastric cancer treatment. Therefore, further studies were designed to explore the mechanisms of actions of PD in AGS cells.

The elucidation of the apoptotic mechanism that PD induces in AGS cells is a very important step in the drug development process. We preliminarily verified that PD promotes an increase in nuclei with apoptotic bodies and nuclear condensation, DNA fragmentation ladders, PS externalization, and the ratio of sub-G1 cells (Figs. 1 and 2). In addition, PD treatment induced morphological changes and rearrangements in AGS cells, which became rounded and eventually detached from the substrate. While they were not detected in the control group, rounded and detached cells were significantly increased in PD-treated groups. The rounded cells were macroscopically obvious following 6–12 h of PD exposure, and the detached cells were observed after 24 h of PD exposure, paralleling the morphological changes observed in anoikis [Kaur, 2006]. However, we did not observe apoptotic effects in the rounded but still adherent cells following 24 h of PD exposure (Fig. 3C). Thus, PD disrupted adhesion signals and promoted anoikis, a specific type of apoptosis induced by cell detachment from the ECM.

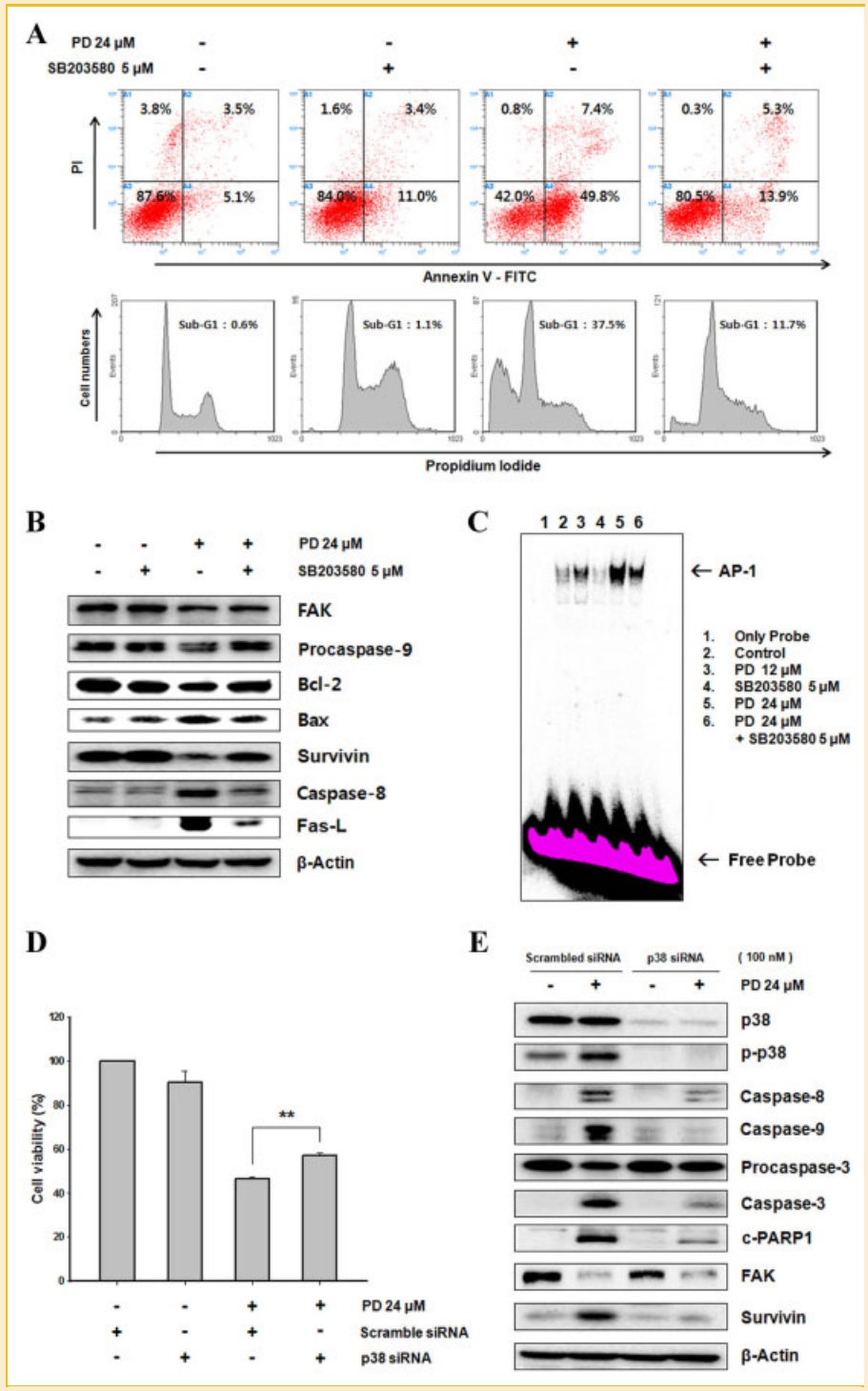

Fig. 6. Effects of the p38 MAPK on PD-induced apoptosis in AGS cells. A: Quantitative analysis of PD-induced apoptosis by Annexin V/PI staining and cell cycle analysis. SB203580 was applied for 1 h before treatment with 24 μM PD or vehicle for 24 h. B: Cell lysates were subjected to Western blotting using the following apoptosis-related proteins antibodies: FAK, caspase-8, caspase-9, Bcl-2, Bax, Survivin, and Fas-L. C: Effects of SB203580 on AP-1 activation by PD. Cells were treated with 12, and 24 μM PD for 24 h. SB203580 was applied for 1 h before treatment with 24 μM PD or vehicle for 24 h. EMSA was performed using nuclear extracts from AGS cells. Data are representative of three independent experiments. D,E: AGS cells were transfected with control scrambled siRNA or p38-alpha MAPK siRNA for 48 h. The transfected cells were then treated with 24 μM PD for 24 h. The cell viability assay (D), and Western blotting (E) were performed.

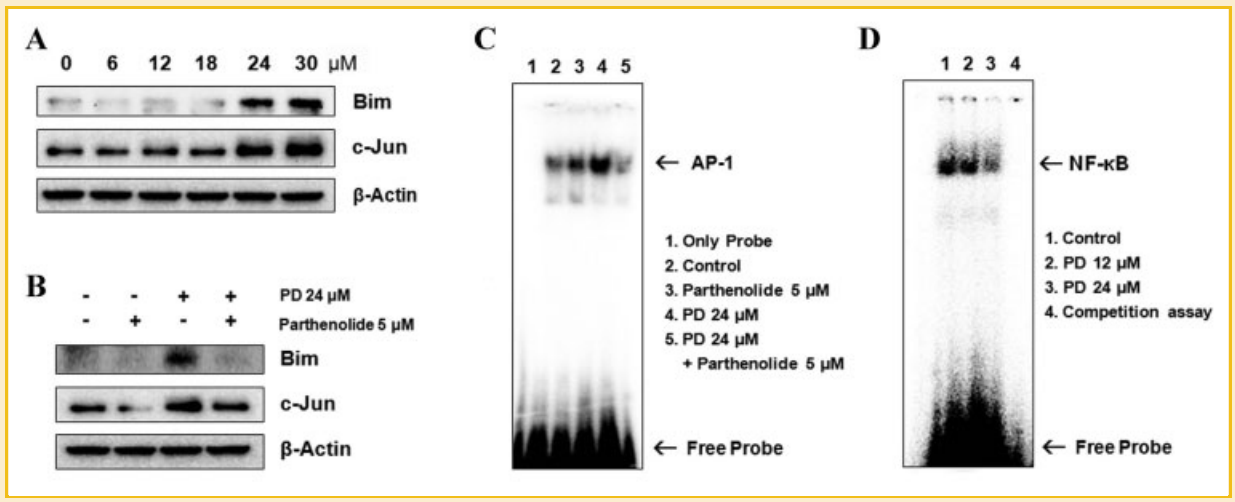

Fig. 7. Effects of the transcription factors AP-1 and NF-κB on PD-induced apoptosis in AGS cells. A: Cell lysates were prepared and subjected to SDS–PAGE and Western blotting to determine the effects of PD on AP-1 transcriptional targets such as c-Jun and Bim. B, C: The effects of pretreatment with parthenolide on the levels of c-Jun and Bim and the activation of AP-1. The protein expression levels were determined using Western blotting (B), and EMSA (C) was performed using nuclear extracts from cells. D: The nuclear extracts were incubated with a ^{32}P-labeled NF-κB consensus oligonucleotide and EMSA was performed.

Apoptosis can be triggered by the extrinsic pathway and intrinsic pathways [Fulda and Debatin, 2006]. When a death receptor such as Fas triggers the extrinsic pathway, Fas-L interacts with the inactive Fas complexes and forms the death-inducing signaling complex. On the other hand, the intrinsic pathway is regulated by the Bcl-2 family members, which can promote cell survival through proteins such as Bcl-2, and Bcl-X_L, or cell death through proteins such as Bax, Bid, Bim, Bad, and Bak [Pan et al., 2008]. In our results, PD increased the expression of Fas-L protein and mRNA levels, suggesting that PD induced apoptosis by inducing both the synthesis and cell surface localization of Fas-L, which binds to Fas and activates caspase-8. The observed increase in expression of Fas-L and cleaved caspase-8 in the PD-treated AGS cells suggests the involvement of the extrinsic pathway.

We also found an increased level of the pro-apoptotic protein Bax and a reduction in the expression of the anti-apoptotic protein Bcl-2 in PD-treated AGS cells. It is well known that the Bcl-2 family proteins such as Bcl-2, and Bax play a crucial role in apoptosis induction [Arnoult et al., 2002]. The increased ratio of Bax: Bcl-2 would elicit the loss of mitochondrial membrane potential and cytochrome *c* release (Fig. 4C,D), which is associated with the activation of caspase-9. Additionally, PD-induced Bid cleavage suggests that cross-talk may exist between the two pathways mediated by caspase-8, which can promote the activities of pro-apoptotic Bcl-2 family proteins and activate caspase-9. These results indicate that PD increases apoptosis in AGS cells through both the extrinsic pathway mediated by caspase-8 activation and the intrinsic pathway mediated by caspase-9 activation, thus ultimately activating the common downstream apoptosis effector caspase-3 (Fig. 3D). In contrast, our data suggest that p53 and p21 are not required for the PD-induced effects in AGS cells (Fig. 3E).

An understanding of MAPK signaling may provide us with important information regarding the chemical-triggered apoptotic processes. Specifically, the activation of p38 MAPK affects the apoptotic pathway either directly by phosphorylation or indirectly by decreasing the expression of the Bcl-2 protein [Chiu et al., 2010]. On the other hand, ERK, activated by growth factors and cytokines, is crucial for cell proliferation and has been shown to suppress apoptosis. Here, we showed that the phosphorylation of p38, and JNK were increased after PD treatment in a dose- and time-dependent manner, but the phosphorylation of ERK was decreased (Fig. 5A). This event was followed by the activation of a caspase cascade, suggesting that p38 and JNK acted upstream of the apoptosis pathway [Park et al., 2010]. To further determine whether the phosphorylation of MAPK family members is associated with PD-induced apoptosis, we used p38, JNK and ERK inhibitors. PD-induced apoptosis was attenuated by the p38 inhibitor SB203580 and promoted by the ERK inhibitor U0126 but was not affected by the JNK inhibitor SP600125, as evidenced by caspase-3 activation and PARP1 cleavage. These results suggest that the activation of p38 MAPK signaling, but not JNK or ERK1/2, is a necessary step in PD-induced apoptosis in AGS cells. Notably, our results show that ERK is involved in PD-induced apoptosis and that an ERK inhibitor might synergistically inhibit cell proliferation (Fig. 5C).

The effect of apoptosis induction by p38 activation was clarified by the reduction of PS externalization and cells in the sub-G1 phase as well as an attenuation of apoptosis-related protein activation. Thus, the activation of p38 was responsible for the PD-induced Bcl-2/Bax modulation, Fas-L up-regulation, caspase-8/-9 activation, and subsequent apoptosis, as shown by the reduction in the presence of the p38 inhibitor SB203580 (Fig. 6A,B). This induction of apoptosis may be associated with anoikis mediated by the detachment-dependent p38 MAPK-driven up-regulation of Fas-L [Puviani et al., 2003; Rosen et al., 2002]. In addition, the PD-induced decrease in FAK expression was not affected by the p38 inhibitor or

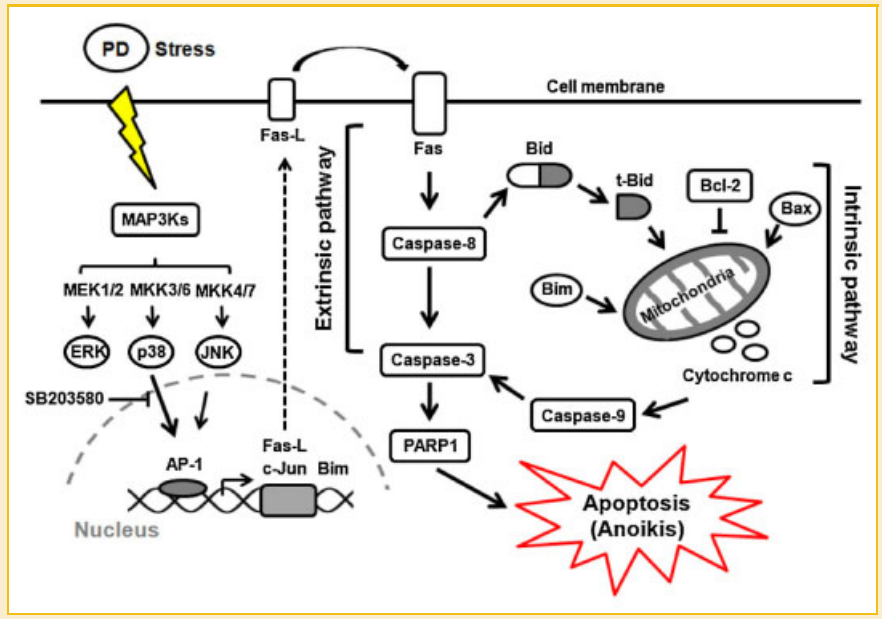

Fig. 8. A schematic model of the biochemical pathway associated with PD-induced apoptosis (anoikis). According to this model, when AGS cells are exposed to PD, a death signal is transduced from the cell membrane to the nucleus through the p38 MAPK and AP-1 signaling pathway. Once p38 MAPK is phosphorylated, it triggers the activation of both extrinsic and intrinsic pathway initiators, caspase-8 and caspase-9. Both pathways converge at the effecter caspase-3, the activation of which eventually executes apoptotic cell death.

p38 siRNA. It would be the reason that the p38 MAPK is an important downstream target of FAK [Boosani et al., 2009].

AP-1, the transcription factor regulated by MAPK regulates the genes involved in cell proliferation, apoptosis, and differentiation in response to external stimuli [Jiang et al., 2001; Silvers et al., 2003]. AP-1 has been proposed to play important roles in carcinogenesis and cancer development. It is well known that Bim and c-Jun, transcriptional targets of AP-1, play a crucial role in the induction of apoptosis [Lauricella et al., 2006]. Bim results in the activation of the intrinsic pathway by interacting with pro-apoptotic protein Bax or anti-apoptotic protein Bcl-2 [Ameyar et al., 2003]. Induction of c-Jun mediated by AP-1 activation has also been linked to apoptosis by repressing the expression of proteins associated with cell survival [Bossy-Wetzel et al., 1997]. We report, for the first time, that PD activates AP-1 transcriptional activity in AGS cells (Fig. 5B). The AP-1 activity inhibited by pretreatment with SB202190 shows that p38 triggers the upstream signaling pathway that regulates the AP-1 DNA-binding activity (Fig. 6C).

In conclusion, our results indicate that PD potentiates the apoptotic effect in AGS human gastric cancer cells. PD induced p38 MAPK activation and led to apoptosis (anoikis) following the detachment of the cells (Fig. 8). These findings will provide important information for the development of PD-derived drugs in AGS cells. In addition, we intend to demonstrate the pharmacological effect and safety profile of PD in a xenograft nude mouse model. These advanced studies are expected to give us important information regarding the use of PD as a candidate therapeutic agent against cancer. In this regard, PD could be of great potential in the treatment of gastric cancer in the near future.

ACKNOWLEDGMENTS

This work was supported by the National Research Foundation of Korea (NRF) grant funded by the Korean government (MEST) (No. 20090083533).

REFERENCES

Ahn KS, Hahn BS, Kwack KB, Lee EB, Kim YS. 2006. Platycodin D-induced apoptosis through nuclear factor-κB activation in immortalized keratinocytes. Eur J Pharmacol 537:1–11.

Ahn KS, Noh EJ, Zhao HL, Jung SH, Kang SS, Kim YS. 2005. Inhibition of inducible nitric oxide synthase and cyclooxygenase II by *Platycodon grandiflorum* saponins via suppression of nuclear factor-κB activation in RAW 264.7 cells. Life Sci 76:2315–2328.

Ameyar M, Wisniewsk M, Weitzman JB. 2003. A role for AP-1 in apoptosis: The case for and against. Biochimie 85:747–752.

Arnoult D, Parone P, Martinou JC, Antonsson B, Estaquier J, Ameisen JC. 2002. Mitochondrial release of apoptosis-inducing factor occurs downstream of cytochrome *c* release in response to several proapoptotic stimuli. J Cell Biol 159:923–929.

Boosani CS, Nalabothula N, Munugalavadla V, Cosgrove D, Keshamoun VG, Sheibani N, Sudhakar A. 2009. Fak and p38-MAP kinase-dependent activation of apoptosis and caspase-3 in retinal endothelial cells by α1 (IV)NC1. Invest Ophthalmol Vis Sci 50:4567–4575.

Bossy-Wetzel E, Bakiri L, Yaniv M. 1997. Induction of apoptosis by the transcription factor c-Jun. EMBO J 16:1695–1709.

Boulares AH, Yakovlev AG, Ivanova V, Stoica BA, Wang G, Iyer S, Smulson M. 1999. Role of poly (ADP-ribose) polymerase (PARP) cleavage in apoptosis. J Biol Chem 274:22932–22940.

Chang L, Karin M. 2001. Mammalian MAP kinase signalling cascades. Nature 410:37–40.

Chin YW, Balunas MJ, Chai HB, Kinghorn AD. 2006. Drug discovery from natural sources. AAPS J 8:239–253.

Chiu CC, Chen JYF, Lin KL, Huang CJ, Lee JC, Chen BH, Chen WY, Lo YH, Chen YL, Tseng CH, Chen YL, Lin SR. 2010. p38 MAPK and NF-κB pathways are involved in naphtho [1,2-b] furan-4,5-dione induced anti-proliferation and apoptosis of human hepatoma cells. Cancer Lett 295:92–99.

Cragg GM, Grothaus PG, Newman DJ. 2009. Impact of natural products on developing new anti-cancer agents. Chem Rev 109:3012–3043.

Frisch SM, Screaton RA. 2001. Anoikis mechanisms. Curr Opin Cell Biol 13:555–562.

Fulda S, Debatin K. 2006. Extrinsic versus intrinsic apoptosis pathways in anticancer chemotherapy. Oncogene 25:4798–4811.

Fulop T, Larbi A. 2002. Putative role of 67 kDa elastin-laminin receptor in tumor invasion. Semin Cancer Biol 12:219–229.

Ghobrial IM, Witzig TE, Adjei AA. 2005. Targeting apoptosis pathways in cancer therapy. CA Cancer J Clin 55:178–194.

Giancotti FG, Ruoslahti E. 1999. Integrin signaling. Science 285:1028–1032.

Giuliano M, Calvaruso G, Pellerito O, Portanova P, Carlisi D, Vento R, Tesoriere G. 2006. Anandamide-induced apoptosis in Chang liver cells involves ceramide and JNK/AP-1 pathway. Int J Mol Med 17:811–819.

Gordaliza M. 2007. Natural products as leads to anticancer drugs. Clin Transl Oncol 9:767–776.

Ha YW, Kim YS. 2009. Preparative isolation of six major saponins from Platycodi Radix by high speed counter current chromatography. Phytochem Anal 20:207–213.

Jiang XH, Wong B, Lin M, Zhu GH, Kung HF, Jiang SH, Yang D, Lam SK. 2001. Functional p53 is required for triptolide-induced apoptosis and AP-1 and nuclear factor-kappaB activation in gastric cancer cells. Oncogene 20:8009–8018.

Johnson GL, Lapadat R. 2002. Mitogen-activated protein kinase pathways mediated by ERK, JNK, and p38 protein kinases. Science 298:1911–1912.

Kaufmann SH, Earnshaw WC. 2000. Induction of apoptosis by cancer chemotherapy. Exp Cell Res 256:42–49.

Kaur M. 2006. Grape seed extract induces anoikis and caspase-mediated apoptosis in human prostate carcinoma LNCaP cells: Possible role of ataxia telangiectasia mutated-p53 activation. Mol Cancer Ther 5:1265–1274.

Kim MO, Moon DO, Choi YH, Lee JD, Kim ND, Kim GY. 2008a. Platycodin D induces mitotic arrest in vitro, leading to endoreduplication, inhibition of proliferation and apoptosis in leukemia cells. Int J Cancer 122:2674–2681.

Kim MO, Moon DO, Choi YH, Shin DY, Kang HS, Choi BT, Lee JD, Li W, Kim GY. 2008. Platycodin D induces apoptosis and decreases telomerase activity in human leukemia cells. Cancer Lett 261:98–107.

Lauricella M, Emanuele S, D'Anneo A, Calvaruso G, Vassallo B, Carlisi D, Portanova P, Vento R, Tesoriere G. 2006. JNK and AP-1 mediate apoptosis induced by bortezomib in HepG2 cells via FasL/caspase-8 and mitochondria-dependent pathways. Apoptosis 11:607–625.

Lee H, Kang R, Kim YS, Chung SI, Yoon Y. 2010. Platycodin D inhibits adipogenesis of 3T3 L1 cells by modulating kruppel like factor 2 and peroxisome proliferator activated receptor gamma. Phytother Res 24:161–167.

Lee KW, Kim SG, Kim HP, Kwon E, You J, Choi HJ, Park JH, Kang BC, Im SA, Kim TY, Kim WH, Bang YJ. 2008. Enzastaurin, a protein kinase Cβ inhibitor, suppresses signaling through the ribosomal S6 kinase and bad pathways and induces apoptosis in human gastric cancer cells. Cancer Res 68:1916–1926.

Li C, Xu Q. 2000. Mechanical stress-initiated signal transductions in vascular smooth muscle cells. Cell Signal 12:435–445.

Li H, Zhu H, Xu C, Yuan J. 1998. Cleavage of BID by caspase 8 mediates the mitochondrial damage in the Fas pathway of apoptosis. Cell 94:491–501.

Liu MJ, Wang Z, Li HX, Wu RC, Liu YZ, Wu QY. 2004. Mitochondrial dysfunction as an early event in the process of apoptosis induced by Woodfordin I in human leukemia K562 cells. Toxicol Appl Pharmacol 194:141–155.

Mansouri A, Ridgway LD, Korapati AL, Zhang Q, Tian L, Wang Y, Siddik ZH, Mills GB, Claret FX. 2003. Sustained activation of JNK/p38 MAPK pathways in response to cisplatin leads to Fas ligand induction and cell death in ovarian carcinoma cells. J Biol Chem 278:19245–19256.

Naka T, Sugamura K, Hylander BL, Widmer MB, Rustum YM, Repasky EA. 2002. Effects of tumor necrosis factor-related apoptosis-inducing ligand alone and in combination with chemotherapeutic agents on patients' colon tumors grown in SCID mice. Cancer Res 62:5800–5806.

Pan M-H, Ghai G, Ho C-T. 2008. Food bioactives, apoptosis, and cancer. Mol Nutr Food Res 52:43–52.

Park EK, Park MJ, Lee SH, Li YC, Kim J, Lee JS, Lee JW, Ye SK, Park JW, Kim CW. 2009. Cholesterol depletion induces anoikis like apoptosis via FAK down regulation and caveolae internalization. J Pathol 218:337–349.

Park IJ, Kim MJ, Park OJ, Park MG, Choe W, Kang I, Kim SS, Ha J. 2010. Cryptotanshinone sensitizes DU145 prostate cancer cells to Fas (APO1/CD95)-mediated apoptosis through Bcl-2 and MAPK regulation. Cancer Lett 298:88–98.

Parkin DM. 2001. Global cancer statistics in the year 2000. Lancet Oncol 2:533–543.

Puviani M, Marconi A, Cozzani E, Pincelli C. 2003. Fas ligand in pemphigus sera induces keratinocyte apoptosis through the activation of caspase-8. J Invest Dermatol 120:164–167.

Ravindran J, Prasad S, Aggarwal BB. 2009. Curcumin and cancer cells: How many ways can curry kill tumor cells selectively? AAPS J 11:495–510.

Roder DM. 2002. The epidemiology of gastric cancer. Gastr Cancer 5:5–11.

Rosen K, Shi W, Calabretta B, Filmus J. 2002. Cell detachment triggers p38 mitogen-activated protein kinase-dependent overexpression of Fas ligand. J Biol Chem 277:46123–46130.

Shin DY, Kim GY, Li W, Choi BT, Kim ND, Kang HS, Choi YH. 2009. Implication of intracellular ROS formation, caspase-3 activation and Egr-1 induction in platycodon D-induced apoptosis of U937 human leukemia cells. Biomed Pharmacother 63:86–94.

Shin EM, Zhou HY, Xu GH, Lee SH, Merfort I, Kim YS. 2010. Anti-inflammatory activity of hispidol A 25-methyl ether, a triterpenoid isolated from Ponciri Immaturus Fructus. Eur J Pharmacol 627:318–324.

Silvers AL, Bachelor MA, Bowden GT. 2003. The role of JNK and p38 MAPK activities in UVA-induced signaling pathways leading to AP-1 activation and c-Fos expression. Neoplasia 5:319–329.

Tanos T, Marinissen MJ, Leskow FC, Hochbaum D, Martinetto H, Gutkind JS, Coso OA. 2005. Phosphorylation of c-Fos by members of the p38 MAPK family. J Biol Chem 280:18842–18852.

Varadhachary GR, Ajani JA. 2005. Gastric cancer. Clin Adv Hematol Oncol 3:118–124.

Wagner EF, Nebreda AR. 2009. Signal integration by JNK and p38 MAPK pathways in cancer development. Nat Rev Cancer 9:537–549.

Wang C, Schuller Levis, GB, Lee EB, Levis WR, Lee DW, Kim BS, Park SY, Park E. 2004. Platycodin D and D3 isolated from the root of *Platycodon grandiflorum* modulate the production of nitric oxide and secretion of

TNF-α in activated RAW 264.7 cells. Int Immunopharmacol 4:1039–1049.

Windham TC, Parikh NU, Siwak DR, Summy JM, McConkey DJ, Kraker AJ, Gallick GE. 2002. Src activation regulates anoikis in human colon tumor cell lines. Oncogene 21:7797–7807.

Yan H, Zhu Y, Liu B, Wu H, Li Y, Wu X, Zhou Q, Xu K. 2011. Mitogen-activated protein kinase mediates the apoptosis of highly metastatic human non-small cell lung cancer cells induced by isothiocyanates. Br J Nutr 106: 1–13.

Yu JS, Kim AK. 2010. Platycodin D induces apoptosis in MCF-7 human breast cancer cells. J Med Food 13:298–305.

Zhao HL, Cho KH, Ha YW, Jeong TS, Lee WS, Kim YS. 2006. Cholesterol-lowering effect of platycodin D in hypercholesterolemic ICR mice. Eur J Pharmacol 537:166–173.

Zouq NK, Keeble JA, Lindsay J, Valentijn AJ, Zhang L, Mills D, Turner CE, Streuli CH, Gilmore AP. 2009. FAK engages multiple pathways to maintain survival of fibroblasts and epithelia-differential roles for paxillin and p130Cas. J Cell Sci 122:357–367.